

Synthesis of Silver Nanoparticles and Forced Convective Heat Transfer Coefficient Measurement of Silver-Water Nanofluids at Laminar Flow

Research Article

Muhammad Zamir Hossain^{1,*}, Bodrun Nahar¹, Biswajit Kumar Biswas¹, Momotaj Easmin¹, Sanjoy Halder¹ and Md. Abdul Gafur²

¹Department of Chemistry, Jagannath University, Dhaka-1100, Bangladesh

²Bangladesh Council of Scientific and Industrial Research, Dhaka-1205, Bangladesh

DOI: <https://doi.org/10.3329/jnujsci.v11i1.76689>

Received: 12 November 2023, Accepted: 5 March 2024

ABSTRACT

Heat management in industries and other areas is a major issue currently worldwide. Conventional heat transfer fluids like water and ethylene glycol are not very effective. Nanofluids (NFs), composed of nanoparticles (NPs) dispersed throughout a base fluid (BF), have recently been identified as promising heat management agents for various industrial and other applications. Heat transmission is one of the many uses for AgNPs–water NFs (silver NPs (AgNPs) dispersed in water). The goal of this work was to determine the AgNPs–water NFs' forced convective heat transfer coefficient (HTC) in laminar flow. Due to this, we present the results of the HTC study of AgNPs–water NFs in laminar flow in this paper. First, using AgNO₃ as a precursor, a chemical reduction approach was used for facile synthesis of AgNPs in one pot at ambient temperature. Synthesized NPs were examined using ultraviolet-visible spectroscopy (UV-vis), X-ray diffraction (XRD), and transform electron microscopy (TEM) techniques. The average particle size obtained from TEM is 25 nm. The required quantity of AgNPs was added to the water to produce 0.5 and 1.0 vol% of AgNPs–water NFs. Next, zeta potential and dynamic light scattering (DLS), in addition to time-lapse observation and captured picture comparison, were used to assess the stability of the formulated NFs. To calculate the forced convective HTC of prepared NFs in laminar flow, a vertical shell and tube heat transfer apparatus and computer-based data recorder were used. According to the results, in comparison to BF, the HTC of 0.5 and 1.0 vol% NFs was 3.3 and 5 times greater, respectively which encourages the use of AgNPs–water NFs in industry and other heat management.

Keywords: Heat management, Heat transfer coefficient, Laminar flow, Silver-water nanofluids, Stability

*Corresponding Author: Muhammad Zamir Hossain

E-mail: zamir@chem.jnu.ac.bd

1. Introduction

Industrial and other heat management is an important issue currently worldwide. Inefficiency and poor HTC of conventional fluids like water, oil, and ethylene glycol make them undesirable for heat management. In recent decades, NFs have been considered excellent alternatives to conventional heat transfer fluids (water, ethylene glycol, etc.) for industrial and other heat management. NFs are the colloidal dispersion of NPs in BFs and were first invented by Choi (Choi, 1995). NFs offer a variety of new applications in industrial and other heat management such as in power generation by solar and nuclear energy, electronics cooling, refrigeration, and others (Li et al., 2016), (Hamad et al., 2021), (Tripathi & Bég, 2014), (Wahab et al., 2019). The possible areas of NFs applications are increasing with the increased magnitude of research. Therefore, it is expected that NFs will be more lucrative materials for various fields shortly. Silver–water NFs have many possibilities for lucrative applications. Particularly, silver–water NFs may enhance heat transfer. However, HTC measurement is needed to assess the heat transfer (HT) ability of AgNPs–water NFs.

HT measurement of silver-water NFs was surveyed and the current scenario of the present research area is summarized in this section. According to the survey, an experimental investigation to examine the properties of the HT of silver/water NFs was performed by Godson et al. using a shell and tube heat exchanger for a test matrix designed in the turbulent domain, with a variable Reynolds number ranging from 5000 to 25000. Particle volume concentrations were 0.01, 0.03, and 0.04%, and a variable heat flux originating from a solar flat plate collector ranged from 800 W/m² to 1000 W/m². A maximum of 12.4% of enhancement of HTC was observed (Godson et al., 2014). Another experimental study of heat transmission in automobile radiators using silver/water NFs revealed that the HT efficiency increases by up to 30.2% compared to water (Jarrah et al., 2021).

Selvam et al. reported the convective HT properties of water–ethylene glycol mixed fluids seeded with silver NFs in laminar, transitional, and turbulent regimes using the volume concentrations of 0.05, 0.1, 0.15, 0.3, and 0.45% of silver NPs. Thermophysical property measurements were performed using standard methods, including thermal conductivity, viscosity, density, and specific heat capacity. In a tube-in-tube counterflow heat exchanger, convection experiments were performed with NFs serving as the heated medium (Selvam et al., 2016). Also, the effect of silver-water NFs on the heat transfer performance of plate heat exchangers (PHE) was performed by Pourhoseini et al. both experimentally and theoretically. The authors proposed a simple preparation method for silver-water NFs and measurement of their HTC by the PHE. The results show that PHE's overall HTC is improved by both NF concentration and volume flow rate. There is a critical concentration for NF (2.5 mg/L), at which the rate of HT reaches its maximum value (Pourhoseini et al., 2018). Additionally, several theoretical works have been found to calculate the HTC of silver-water NFs (Khodabandeh et al., 2021), (Khodabandeh et al., 2021). Most of the HTC measurements, however, were performed in turbulent flow regimes (Safaei et al., 2016). For instance, Iyahrja et al. assessed the HT of silver-water NFs in a circular tube at turbulent flow (Iyahrja et al., 2018). HT performance of silver water NFs in a solar flat plate was also investigated by Roy et al. applying the Reynolds number between 500 and 25000 (Roy et al., 2015). Very few papers focused on the convective HTC of silver-water NFs using vertical tube and shell tube apparatuses in the laminar flow. Therefore, HTC measurement of AgNPs-water NFs with a vertical shell and tube at a laminar flow apparatus would be worthy.

AgNPs–water NFs preparation is the first task as a means of HTC measurement. To do so, AgNPs need to be synthesized in the beginning. AgNPs can

be synthesized through some methods including chemical, physical, and biological (Syafiuddin et al., 2017). Due to its simplicity and convenience in producing AgNPs, the chemical approach is the most popular among those (Tran et al., 2018). Because, the chemical approach has various benefits over other approaches, including the need for straightforward instruments, affordability from an economic standpoint, rapid reaction times, and high yield %. In particular, AgNPs can be synthesized by chemical reduction method easily (Hossain et al., 2018). Silver nitrate, hydrazine, trisodium citrate (TSC), and water are used as precursors (P), reducing agents (RA), capping agents (CA), and reaction media, respectively, in the majority of chemical reduction procedures to synthesize AgNPs (Syafiuddin et al., 2017). The reduction of silver nitrate results in the synthesis of AgNPs, which goes through multiple steps including atomization (from silver ion), aggregation, nucleation, and particle development and formation. The formation of AgNPs can be confirmed by some characterization techniques.

Next, preparation and stability assessment of NFs is needed. NF preparation method has great importance because it does not mix solid particles in a liquid. The two-step procedure is typically used to prepare NFs, first synthesizing NPs and then distributing them in BFs to produce NFs. For feasibility, the one-step method is also used in which the NPs synthesis and NF preparation are done in a single step (Sidik et al., 2014).

Stability assessment of the prepared NF is important for any application. Stable NFs allow their applications in a variety of fields. Stability can be assessed primarily by naked-eye observation of clear solution, agglomeration, or sedimentation of NFs (Ilyas et al., 2014). Because rapid sedimentation indicates the instability of the prepared NFs. Often, NPs tend to agglomerate and make clusters and become larger in size and then, sediment at the bottom of the container which can

be seen in a transparent glass vial. The stability of NFs can also be evaluated by comparing the images captured using a camera. One of the good options to check the stability is the measurement of zeta potential. Typically, the zeta potential value from +60 mV to -60 mV of an NF indicates stability. NFs with zeta potential values greater than +60 mV or lower than -60 mV are frequently unstable (Sati et al., 2018). Another approach for NFs' stability assessment is DLS measuring using light scattering theory. DLS provides the diameter of particle size in liquid which can be compared with the diameter of pristine particle size. Sizes of NPs in liquids can indicate whether the NF is stable or not. In this way, the stability of the prepared NFs can be evaluated.

In the end, for the HTC measurement of AgNPs–water NFs, the geometry of equipment is important. HTC measurements require various instruments with different geometries depending on the requirements of application areas. Previously, the HTC of different NFs was measured using a vertical Shell and Tube apparatus (Luna et al., 2015) (Alam et al., 2022).

In this paper, we synthesized TSC-coated AgNPs from AgNO₃ and tested the stability of 0.5 and 1.0 vol% AgNPs–water NFs using sedimentation observation, zeta potential, and DLS. Finally, the HTC of AgNPs–water NFs was measured.

2. Materials and Method

2.1 Materials

Silver nitrate (AgNO₃, purity 99.5%,) and hydrazine hydrate (H₄N₂·H₂O, purity 80%) were used as a precursor and reducing agent, respectively. Both the materials were purchased from Sigma-Aldrich, Germany, and used as received. Trisodium citrate (TSC, purity 97%), a capping agent, was purchased from Merck, India. All the chemicals were reagent grade. De-ionized water (DIW) was used as a solvent for all solution preparation and NFs preparation.

2.2 Synthesis of TSC-coated AgNPs

Following the method described below, AgNPs were synthesized using a chemical reduction technique (Halder et al., 2021). TSC, hydrazine, and AgNO₃ were used as a capping agent, reducing agent, and precursor for the synthesis of AgNPs. To synthesize TSC-covered AgNPs, typically 50 mL of 0.001 mmolL⁻¹ AgNO₃ aqueous solution is prepared by dissolving the requisite amount of AgNO₃ salt into DIW. Separately, an aqueous hydrazine solution was made in DIW. After combining the two solutions, TSC was added dropwise with magnetic stirring. Following consideration of the capping agent's ratio's effects, the molar ratios of the precursor, reducing agent, and capping agent were decided to be 1:3:6. The solution was then vigorously agitated for 4 hours. Black coloration may initially be noticeable. After the reaction was finished, the solution took on a brownish-yellowish hue, indicating the formation of AgNPs. AgNPs are produced as colloidal dispersions in a mixture of water, unreacted hydrazine, and the precursor solution. The solid NPs were collected for analytical purposes. By centrifuging the solution at 8000 rpm for 15 minutes, water, the unreacted hydrazine, and unreacted silver ions (if any) were eliminated. The product was re-dispersed in water and collected after centrifuging the particles at 8000 rpm for 15 minutes. To properly purify the products, the procedure was repeated, followed by oven drying. Centrifuged and collected materials are dried in an oven at 105 °C for several hours. The synthesized compounds were then kept in desiccators for subsequent analysis.

2.3 Analysis of the Synthesized AgNPs

Using a spectrophotometer (UV-1800, Shimadzu, Japan) with a variable wavelength range of 200 nm to 800 nm in quartz cuvettes having a path length of 10 mm, a UV-vis spectrum was acquired to obtain a preliminary understanding of whether the AgNPs were created or not. Using a SmartLab 9MTP X-ray diffractometer from Rigaku Corporation and CuK

radiation in a 2θ configuration, the crystallinity of the produced products was evaluated. A scanning speed of 0.02 Hz/0.6 s was used to scan the 2° angle between 30 and 90°. The measured data were compared to the data from the silver file (File No. 00-004-0783) from the Joint Committee for Powder Diffraction Studies (JCPDS). Debye-Shreerer's equation and the two essential peak patterns were used to determine the average crystallite size. Based on Debye-Shreerer's equation and the two essential peak patterns, the average crystallite size was determined. With the use of a transmission electron microscope (TEM, HD 2700, Hitachi Corporation, Japan) with a 200 kV acceleration voltage, particle size, shape, and morphology were studied. 100 particle' sizes were measured in the TEM images to determine the mean particle size.

2.4 Preparation and Stability Assessment of AgNPs–water NFs

After the synthesis of a typical batch, first, AgNPs were first dried (at 105 °C) in the oven, and the weight was recorded. Similarly, we took the weight of 10 batches of AgNPs, and the average weight was obtained as 16 mg. The product of every single batch (16 mg) was used to prepare AgNPs–water NFs. In this case, AgNPs were not dried before the preparation of NFs. Rather, after washing and centrifugation, the required amount of batches of the product was dispersed in 100 mL of DIW. Thus, 0.5 vol% and 1.0 vol% of AgNPs–water NFs were prepared. This NFs preparation is similar to the two-step method. The following equation (1) is used to calculate the volume % of the AgNP–water NFs.

$$\text{Vol}\%, \Phi = \left[\frac{\left(\frac{W_{Ag}}{\rho_{Ag}} \right)}{\left(\frac{W_{Ag}}{\rho_{Ag}} + \frac{W_{bf}}{\rho_{bf}} \right)} \right] \times 100 = \left[\frac{\left(\frac{W_{Ag}}{10.800} \right)}{\left(\frac{W_{Ag}}{10.800} + \frac{10}{1000} \right)} \right] \times 100 \quad (1)$$

Here, Φ is volume fraction (%), W_{Ag} =weight of Ag, ρ_{Ag} =density of Ag, W_{bf} =weight of BF, ρ_{bf} =density of bf.

As mentioned earlier, AgNPs–water NF was prepared in two steps. That means NPs were

synthesized, washed, purified, centrifuged, and collected. Then, for NFs preparation, centrifuged NPs are re-dispersed in water, and NFs are prepared. The NFs preparation does not require any further treatment. A UV-1800 spectrophotometer from Shimadzu, Japan, with a variable wavelength between 200 nm and 800 nm, along with quartz cuvettes with a 10 mm path length, was used to perform the stability assessment of the nanofluid at room temperature. A Zeta seizer ZS-nano Malvern is also used by DLS to measure zeta potential and zeta size.

2.5 HTC Measurement of AgNPs–water NFs

The convective HTC of the NFs was ascertained using an experimental setting. The experimental setup is shown schematically in Figure 1. In the experimental setting, hot water was maintained at a constant temperature of 100 °C in a 350 mL reservoir shell. For certain measurements, hot water was also maintained at a constant temperature of 55, 65, and 75 °C. Immiscible heaters (Watlow ref. L14JX8B) with a 2 kW output are fitted in the shell to heat the water. The heat flux was kept going at a steady pace. Incorporated inside the shell was a spiral tube constructed of smooth copper tubing with a 0.44×10^{-3} m outer diameter, 0.15×10^{-3} m thickness, 0.29×10^{-3} m inner diameter, and a heat exchange length of 0.6858 m. A spiral tube made of smooth copper tubing that had an inner diameter of 0.29 m, an outside diameter of 0.44 m, and a heat exchange length of 0.6858 m was integrated into the shell. Using a centrifugal pump (Espa Ref. XVM8 03F15T), the NFs and BF were collected into a reservoir. There were between 400 and 600 Reynolds numbers in the flow. The NFs and BFs were thereafter allowed to travel through the test area. AgNPs–water NF flow tests were used to confirm laminar flow. We observed the flow after adding some colors to the AgNPs water. No layer alteration or vertical movement of pigments was noticed. The flow was described as laminar in this fashion. The fluids left the tube after absorbing heat from the hot water. As hot liquids passed through the tube, they were collected in a beaker. To

minimize heat loss from the system, the test area is well insulated with glass wool. K-type thermocouples are used to gauge the temperature of the shell and outflow side tube.

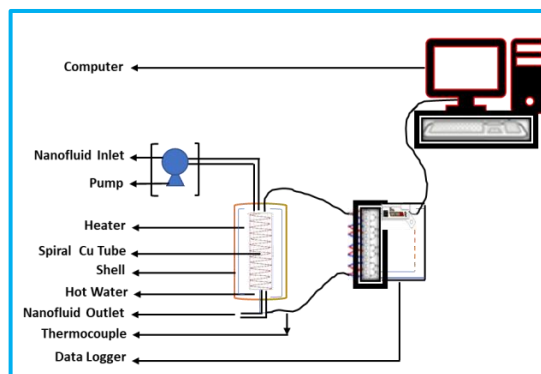


Fig. 1. Setup for the experimental measurement of forced convective HTC of AgNPs–water NFs.

3. Results and Discussion

3.1 Characterization of the Synthesized AgNPs using UV-vis, XDR, and TEM

The absorbance spectra between 200 and 800 nm of aqueous solution of TSC-coated AgNPs are shown in Fig. 2. Characteristic strong absorption peak maxima (λ_{\max}) at 416 nm of wavelength predominantly imply colloidal particle production as a result of surface capping which is close with literature value (Halder et al., 2021).

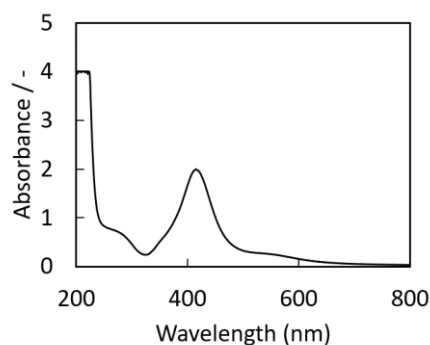


Fig. 2. UV-vis spectrum of the TSC-coated silver NPs.

Figure 3 shows the XRD patterns of synthetic TSC-

coated AgNPs. Five diffraction peaks at (2θ) values of 38.09, 44.27, 64.43, 77.37, and 81.51° which correspond to the (111), (200), (220), (311), and (222) planes of Ag, respectively, are visible in the XRD patterns and demonstrate the crystalline character of the synthesized products of both types. The patterns of the chemically created AgNPs show a spherical structure when compared to JCPDS (File No. 00-004-0783), as shown in Fig. 3.

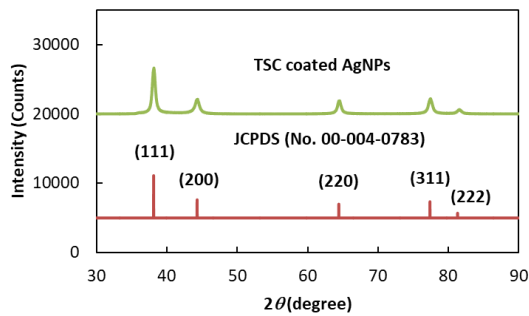


Fig. 3. XRD patterns of the (a) JCPDS file No. 00-004-0783 (b) synthesized TSC-coated AgNPs.

Debye-Scherer's equation was used to calculate the AgNPs' average crystallite size.

$$D = 0.9\lambda/\beta\cos\theta$$

Where D is the mean dimension of the crystallite, β is the full width at half maximum (FWHM) of the diffraction peak, θ is the diffraction angle, and λ is the wavelength of CuK radiation (0.15406 nm), and k is a constant (0.9). By determining the FWHM of the different planes of Bragg's reflection, the estimated average crystallite size was 19 nm.

Figure 4 depicts the TEM images of the TSC-coated AgNPs. Fig. 4 shows that TSC-coated AgNPs show small sizes with spherical shapes. The average particle size obtained from TEM calculation is ~25 nm.

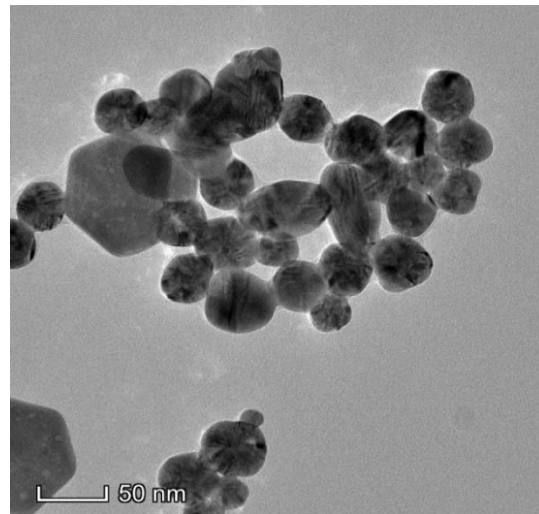


Fig. 4. TEM images of synthesized TSC-coated AgNPs.

3.2 Preparation of AgNPs–water NFs and their Stability Assessment

Figure 5 shows the images of prepared AgNPs–water NFs with concentrations of 0.5 vol% and 1.0 vol%. The color of the 1% AgNP-water NF is different from that of 0.5% because the color changes with the concentration/vol% of AgNPs. It may be due to light scattering. Probably, at higher concentrations agglomeration occurs to some extent, and mie scattering occurs. However, no sedimentation was observed from the image which indicates the stability of the prepared NFs.



Fig. 5. Images of AgNPs–water NFs at different concentrations.

Zeta-potential of the prepared 1.0 vol% AgNPs–water NF was measured at 25 °C using DLS to check the stability of the AgNPs–water NF. Fig. 6 shows the zeta potential of the NF. The obtained zeta potential value from +10 mV to -10 mV i.e. near zero indicates the instability of the NF after the preparation.

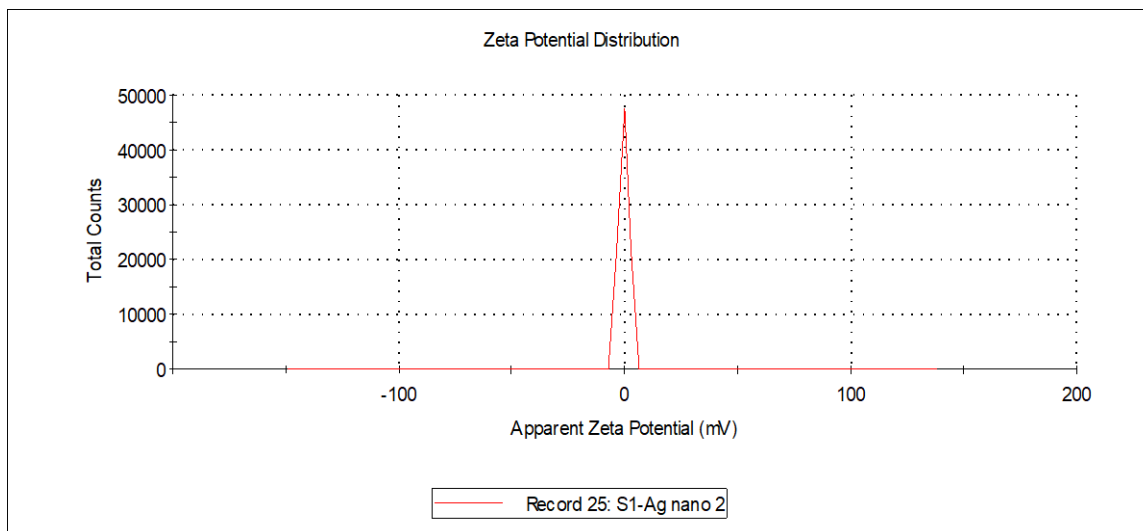


Fig. 6. Zeta-potential of 1.0% AgNF–water NF after its preparation.

Figure 7 shows the DLS size of the NPs in 1.0 vol% AgNPs–water NFs. Fig. 7 indicates that the AgNPs get agglomerated with time increment. The size distribution ranges between 5 to 500 nm. Of

course, most of the particle sizes (84%) remained below 90 nm with an average size of 45 nm as obtained from Fig. 7. This indicates the stability of the prepared NFs to some extent.

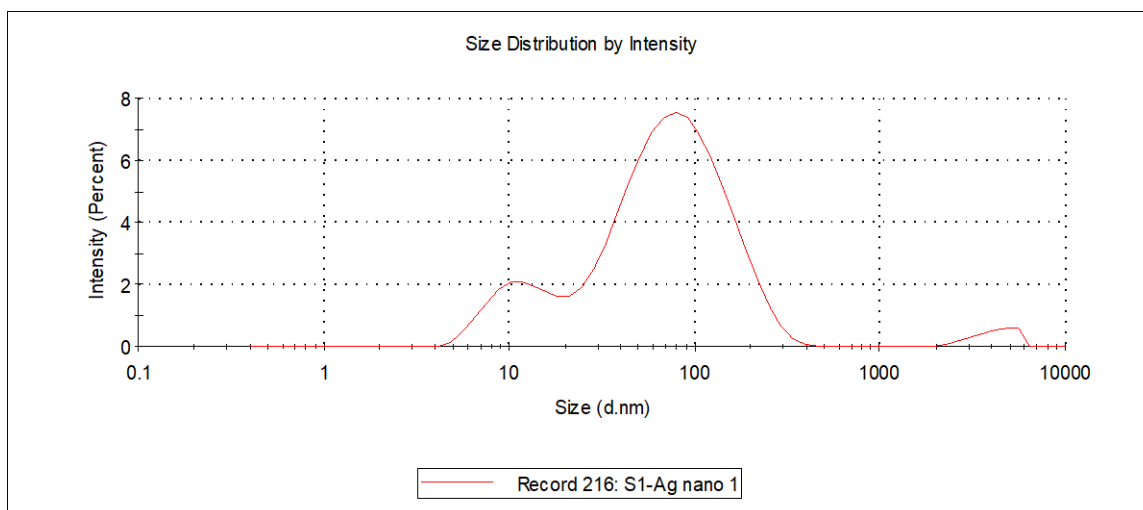


Fig. 7. Particle diameter of 1.0 % AgNPs–water NFs after its preparation.

3.4 HTC measurement of AgNPs-water NFs

Convective HT between a moving fluid and a solid surface can be defined by the following relationship (Alam et al., 2022).

$$Q = hA (T_s - T_f) = hA\Delta T \quad (2)$$

where A is the area of the surface that is in contact with the fluid (m²), Q is the rate of forced convection HT (W), T_s is the solid surface temperature (K), T_f is the fluid temperature (K), and h is the convective HTC (W/m²•K).

$$Q = mS\Delta\theta \quad (3)$$

where m is the hot water's mass in kilograms. Water has a specific heat of J/kg•K, and the

temperature difference between the water before and after it has been released is K.

These connections can be summed up as follows:

$$h = (Q/A)/(\Delta T) = mS\Delta T/(A \cdot \Delta T) \quad (4)$$

Give the BF, 0.5, and 1.0 vol% AgNPs-water NFs a respective HTC of h₀, h₁, and h₂. For the BF, 0.5, and 1.0 vol% AgNPs–water NFs, the temperature difference between the before- and after-release temperatures was set as 0, 1, and 2, respectively. BF, 0.5, and 1.0 vol% AgNPs-water NFs, respectively, are represented by T₀, T₁, and T₂ of the temperature differential between H₂O and each NF after absorption of heat. Table 1 includes an overview of all the calculation's inputs.

Table 1. Summarization of the parameter for HTC of AgNPs–water NFs.

| Parameters | Value |
|--------------------------------------|--------------------------------------|
| Mass of water | 350 g or 0.35 kg |
| Specific heat of water, S | 4178 J/kg•K |
| The outer diameter of the Cu-tube, d | 0.44 mm or 4.4×10 ⁻⁴ m |
| Heat exchange length of Cu-tube, l | 68.58 cm or 68.58×10 ⁻² m |
| $\Delta\theta_0$ | 0.01 K |
| $\Delta\theta_1$ | 1.3 K |
| $\Delta\theta_2$ | 1.3 K |
| ΔT_0 | 13.49 K |
| ΔT_1 | 4.5 K |
| ΔT_2 | 5.9 K |

Under the conditions of laminar flow, three measurements of forced convective HTC of BF and

AgNPs-water NFs at 0.5 and 1.0 vol% were made. In Fig. 8, the collected data is displayed.

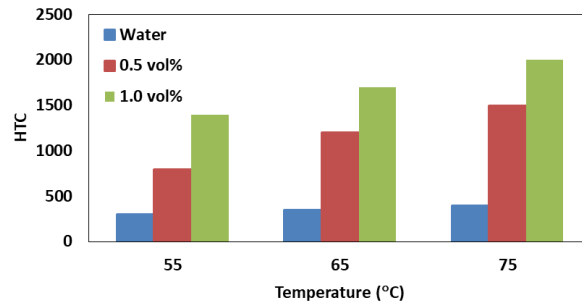


Fig. 8. Forced convective HTC of BF and 0.5 vol% and 1.0 vol% AgNPs–water NFs at different temperatures in laminar flow.

At 55 °C, the calculated forced convective heat transfer coefficients (Wm^2/K) for water with 0.5 and 1.0 vol% of AgNPs-water NFs were 300, 700, and 1400 Wm^2/K , respectively. Forced convective HTC values for water, 0.5 and 1.0 vol% AgNPs-water NFs were 350, 1200, and 1700 Wm^2/K , respectively, at 65 °C. Additionally, the values of the forced convective HTC of water with 0.5 and 1.0 vol% AgNPs-water NFs at 75 °C were computed as 400, 1500, and 2000 Wm^2/K , respectively. At 55 °C, the average forced convective HTC of water with 0.5 and 1.0 vol% AgNPs-water NFs was calculated to be 350, 1167, and 1700 Wm^2/K , respectively. The column graph shows that the HTC values increased as the concentration of NFs increased between 0.5 and 1.0.

Conclusions

The synthesized AgNPs were spherical with an average diameter of 25 nm. AgNPs–water NFs at 0.5 and 1.0 vol% were prepared by dispersing AgNPs to water following two-step method. Image capturing observation of NFs indicates no sedimentation i.e. stability. Zeta potential measurement of 1.0 vol% AgNPs–water nanofluid indicates the instability whereas the DLS size measurement indicated the stability to some extent as some agglomeration occurs. In comparison to water, the HTC of 0.5 and 1.0 vol% AgNPs-water NFs was 3.3 and 5 times greater, respectively. The experimental outcomes showed that the HTC values might be significantly improved by adding tiny amounts of AgNPs.

Acknowledgments

We would like to acknowledge the Ministry of Science and Technology, Bangladesh for providing the fund (No. **39.00.0000.009.14.019.21-Phy's-636/1384**, Date: **15/12/2021**) to perform the research. The authors also acknowledge AIC, Jagannath University for UV-vis, Atomic Energy Centre, Dhaka for providing service to take DLS data (zeta size and zeta potential), Tohoku

University, Japan for TEM analysis, and PP & PDC of BCSIR, Dhaka for instrumental support.

References

- Alam MS, Nahar B, Gafur MA, Seong G, Hossain MZ. 2022. Forced Convective Heat Transfer Coefficient Measurement of Low Concentration Nanorods ZnO–Ethylene Glycol Nanofluids in Laminar Flow. *Nanomaterials*, 12(9). <https://doi.org/10.3390/NANO12091568>
- Choi SUS. 1995. Enhancing thermal conductivity of fluids with nanoparticles. *American Society of Mechanical Engineers, Fluids Engineering Division (Publication) FED*, 231(January 1995), 99–105.
- Godson L, Deepak K, Enoch C, Jefferson Raja BR, Raja B. 2014. Heat transfer characteristics of silver/water nanofluids in a shell and tube heat exchanger. *Archives of Civil and Mechanical Engineering*, 14(3), 489–496. <https://doi.org/10.1016/j.acme.2013.08.002>
- Halder S, Ahmed AN, Gafur MA, Seong G, Hossain MZ. 2021. Size-Controlled Facile Synthesis of Silver Nanoparticles by Chemical Reduction Method and Analysis of Their Antibacterial Performance. *Chemistry Select*, 6(36), 9714–9720. <https://doi.org/10.1002/slct.202101362>
- Hamad EM, Khaffaf A, Yasin O, Abu El-Rub Z, Al-Gharabli S, Al-Kouz W, Chamkha AJ. 2021. Review of Nanofluids and Their Biomedical Applications. *Journal of Nanofluids*, 10(4), 463–477. <https://doi.org/10.1166/jon.2021.1806>
- Hossain MZ, Halder S, Ahmed ANA, Gafur MA. 2018. Synthesis of Spherical Silver Nanoparticles By Chemical Reduction Method. *Journal of Bangladesh Chemical Society*, 30(2), 42–47.
- Ilyas SU, Pendyala R, Marneni N. 2014. Preparation, sedimentation, and agglomeration of nanofluids. *Chemical Engineering and Technology*, 37(12), 2011–2021. <https://doi.org/10.1002/ceat.201400268>
- Iyahraja S, Rajadurai JS, Rajesh S, Pandian RST, Kumaran MS, Selvakumar G. 2018. Studies

- on heat transfer and pressure drop in turbulent flow of silver-water nanofluids through a circular tube at constant wall heat flux. *Heat and Mass Transfer/Waerme-Und Stoffuebertragung*, 54(7), 2089–2099. <https://doi.org/10.1007/s00231-018-2291-9>
- Jarrah HT, Mohtasebi SS, Etefaghi E, Jaliliantabar F. 2021. Experimental investigation of Silver/Water nanofluid heat transfer in a car radiator. *Journal of Mechanical Engineering and Sciences*, 15(1), 7743–7753. <https://doi.org/10.15282/jmes.15.1.2021.10.0610>
- Khodabandeh E, Boushehri R, Akbari OA, Akbari S, Toghraie D. 2021. Numerical investigation of heat and mass transfer of water—silver nanofluid in a spiral heat exchanger using a two-phase mixture method. *Journal of Thermal Analysis and Calorimetry*, 144(3), 1003–1012. <https://doi.org/10.1007/s10973-020-09533-x>
- Li X, Zou C, Chen W, Lei X. 2016. Experimental investigation of β -cyclodextrin modified carbon nanotubes nanofluids for solar energy systems: Stability, optical properties and thermal conductivity. *Solar Energy Materials and Solar Cells*, 157, 572–579. <https://doi.org/10.1016/j.solmat.2016.07.030>
- Luna IZ, Hilary LN, Chowdhury AMS, Gafur MA, Khan N, Khan RA. 2015. Preparation and Characterization of Copper Oxide Nanoparticles Synthesized via Chemical Precipitation Method. *OALib*, 02(03), 1–8. <https://doi.org/10.4236/oalib.1101409>
- Pourhoseini SH, Naghizadeh N, Hoseinzadeh H. 2018. Effect of silver-water nanofluid on heat transfer performance of a plate heat exchanger: An experimental and theoretical study. *Powder Technology*, 332, 279–286. <https://doi.org/10.1016/j.powtec.2018.03.058>
- Roy S, Asirvatham LG, Kunhappan D, Cephas E, Wongwises S. 2015. Heat transfer performance of Silver/Water nanofluid in a solar flat-plate collector. *Journal of Thermal Engineering*, 1(2), 104–112. <https://doi.org/10.18186/jte.29475>
- Safaei MR, Ahmadi G, Goodarzi MS, Shadloo MS, Goshayeshi HR, Dahari M. 2016. Heat transfer and pressure drop in fully developed turbulent flows of graphene nanoplatelets-silver/water nanofluids. *Fluids*, 1(3), 1–12. <https://doi.org/10.3390/fluids1030020>
- Sati P, Shende RC, Ramaprabhu S. 2018. An experimental study on thermal conductivity enhancement of DI water-EG based ZnO(CuO)/graphene wrapped carbon nanotubes nanofluids. *Thermochimica Acta*, 666(June), 75–81. <https://doi.org/10.1016/j.tca.2018.06.008>
- Selvam C, Muhammed Irshad EC, Lal DM, Harish S. 2016. Convective heat transfer characteristics of water-ethylene glycol mixture with silver nanoparticles. *Experimental Thermal and Fluid Science*, 77, 188–196. <https://doi.org/10.1016/j.expthermflusci.2016.04.021>
- Sidik NAC, Mohammed HA, Alawi OA, Samion S. 2014. A review on preparation methods and challenges of nanofluids. *International Communications in Heat and Mass Transfer*, 54, 115–125. <https://doi.org/10.1016/j.icheatmasstransfer.2014.03.002>
- Syafiuddin A, Salmiati Salim MR, Beng Hong Kueh A, Hadibarata T, Nur H. 2017. A Review of Silver Nanoparticles: Research Trends, Global Consumption, Synthesis, Properties, and Future Challenges. *Journal of the Chinese Chemical Society*, 64(7), 732–756. <https://doi.org/10.1002/jccs.201700067>
- Tran QH, Nguyen VQ, Le A. 2018. *Corrigendum : Silver nanoparticles : synthesis, properties, toxicology*. *Adv. Nat. Sci. Nanosci. Nanotechnol.*, 9, 049501.
- Tripathi D, Bég OA. 2014. A study on peristaltic flow of nanofluids: Application in drug delivery systems. *International Journal of Heat and Mass Transfer*, 70, 61–70. <https://doi.org/10.1016/j.ijheatmasstransfer.2013.10.044>
- Wahab A, Hassan A, Qasim MA, Ali HM, Babar H, Sajid MU. 2019. Solar energy systems – Potential of nanofluids. *Journal of Molecular Liquids*, 289. <https://doi.org/10.1016/j.molliq.2019.111049>